Long non-coding RNA MALAT1 promotes cell proliferation, migration and invasion by targeting miR-590-3p in osteosarcoma

HUI ZHAO, YONGPING WANG, WEIHUA HOU, XUANXI DING and WENJI WANG

Department of Orthopedics, First Hospital of Lanzhou University, Lanzhou, Gansu 730000, P.R. China

Received August 3, 2019; Accepted August 9, 2022

DOI: 10.3892/etm.2022.11608

Abstract. Osteosarcoma (OS) is a common malignant bone cancer and commonly occurs in adolescents and children. Long non-coding RNAs (lncRNAs) play major roles in cancer cell proliferation and metastasis. The present study aimed to investigate the potential molecular mechanism of lncRNA MALAT1 in OS. The levels of lncRNA MALAT1 and microRNA-590-3p were detected by reverse transcription-quantitative PCR in OS tissues and cells. Cell Counting Kit-8 and flow cytometry assays were conducted to assess cell proliferation and apoptosis. Cell migration and invasion were examined by Transwell assay. The levels of E-cadherin, N-Cadherin, Vimentin and Snail were measured by western blotting. The target of MALAT1 was predicted using online software and confirmed by luciferase reporter, RNA immunoprecipitation and RNA pull-down assays. The results indicated that MALAT1 was highly expressed in OS tissues and cell lines. MALAT1 knockdown promoted apoptosis and suppressed proliferation, migration, invasion and epithelial-mesenchymal transition (EMT) of OS cells. Overexpression of miR-590-3p increased cell apoptosis and hampered cell proliferation, migration, invasion and EMT in OS cells. In addition, MALAT1 knockdown upregulated the expression of miR-590-3p in OS cells. In conclusion, MALAT1 was demonstrated to suppress cell apoptosis and induce cell proliferation, migration, invasion and EMT by inhibiting miR-590-3p in OS, which indicated that MALAT1 has potential value in the diagnosis and treatment of OS.

Introduction

Osteosarcoma (OS) is a common malignant bone cancer with high aggressiveness and rapid systemic metastasis (1). OS is usually formed in the bones of children and adolescents, with more male than female patients (2). Furthermore, the incidence of OS is high between the ages of 10 and 19 years, with an annual incidence of ~10 patients with OS per million worldwide (3). With the development of surgery and chemotherapy, the 5-year survival rate of patients with OS has reached 60-70% (4). Thus, identifying novel therapies for OS is essential.

Long non-coding RNAs (lncRNAs) are a class of non-coding RNAs of ~200 nucleotides in length that play a critical role in various physiological and pathological processes, including growth, development and oncogenesis (5,6). lncRNAs have been involved in the progression of multiple cancers, including OS (7). A large number of lncRNAs, such as HCG9, MELTF-AS1 and ZEB2-AS1 (8-10), have been found to exert a regulatory effect on cell proliferation, invasion, migration and apoptosis in OS (11). LncRNA MALAT1 is a novel lncRNA that contributes to the occurrence and development of various tumors, including OS (12). Recently, it has been reported that MALAT1 expression is aberrantly regulated in various cancers (13). For instance, previous studies have shown that MALAT1 is upregulated in OS tissues and cells, and promotes OS cell growth and metastasis by binding to microRNA (miRNA/miR)-140-5p or regulating the miR-34a/cyclin D1 axis in OS (14,15).

miRNAs consist of 18-25 nucleotides and are highly conserved short non-coding RNAs. miRNAs have been identified as post-transcriptional regulators in biological and pathological processes (16), including cell proliferation, apoptosis, migration and invasion (17). In addition, a large number of miRNAs have been identified to be associated with cancer. miRNAs act as oncogenes or tumor suppressors by modulating different target mRNAs (18). Previous studies have shown that miR-590-3p plays a role in a variety of tumors. For example, miR-590-3p is a tumor suppressor that inhibits epithelial-mesenchymal transition (EMT) and metastasis of glioblastoma multiforme cells by targeting zinc finger E-box-binding homeobox (ZEB)1 and ZEB2 (19). In breast cancer cells, miR-590-3p suppresses tumor progression by targeting sirtuin 1 (20). Non-coding RNAs including MALAT1, miR-590-3p and TUG1 have been proven to be key regulators of OS (21). The expression level of miR-590-3p in OS tissues and cells is significantly downregulated, and miR-590-3p inhibits the progression of OS by targeting SOX9 (22). However, the relationship between MALAT1 and miR-590-3p in OS progression remains unknown.

Correspondence to: Dr Wenji Wang, Department of Orthopedics, First Hospital of Lanzhou University, 1 Donggang West Road, Lanzhou, Gansu 730000, P.R. China
E-mail: shuawei29601pqi@126.com

Key words: long non-coding RNA MALAT1, microRNA-590-3p, osteosarcoma, proliferation, migration, invasion

The present study discovered that MALAT1 contained some complementary pairing with the seed region of miR-590-3p in 143B and MG-63 cells using bioinformatics analysis. Hence, the study aimed to illuminate whether the involvement of MALAT1 in OS function was mediated by miR-590-3p.

Materials and methods

Tissue samples. A total of 45 pairs of OS tissues and matched adjacent healthy tissues were obtained from patients (30 male patients and 15 female patients; mean age, 22.7±6.18 years) who underwent surgery at First Hospital of Lanzhou University (Lanzhou, China) between June 2018 and March 2021. The inclusion criteria were as follows: i) No other distant metastatic lesions; ii) none of the patients received chemotherapy or radiotherapy prior to surgery; iii) no history of other tumors; iv) patients had complete clinical data. The exclusion criteria were as follows: i) Patients were pregnant or lactating; ii) multiple lesions were present at the first diagnosis; iii) patients had other diseases that would affect the progression of treatment. Written informed consent was obtained from all patients, and the research method was approved by the Ethics Committee of the First Hospital of Lanzhou University (Lanzhou, China). All tissue samples were immediately treated with liquid nitrogen and then stored at -80˚C. A total of 100 mg of each tissue sample was ground in liquid nitrogen for reverse transcription-quantitative (RT-q)PCR.

Cell culture. Human fetal osteoblastic cells (hFOB1.19) and OS cell lines (HOS, U2OS, 143B and MG-63) were obtained from American Type Culture Collection. These cells were cultured in DMEM (Gibco; Thermo Fisher Scientific, Inc.) supplemented with 10% FBS (Gibco; Thermo Fisher Scientific, Inc.), 100 U/ml penicillin and 100 mg/ml streptomycin (Gibco; Thermo Fisher Scientific, Inc.) at 37˚C in a humidified atmosphere with 5% CO_2.

Plasmids and cell transfection. Small interfering RNA (siRNA) against MALAT1 (si-MALAT1: sense strand: 5'-AAGAAA AAUAAAGCUUUCCU-3', antisense strand: 5'-GAAAGC UUUUUAUUUUUCUUCC-3') and corresponding negative control siRNA (Scramble: sense strand: 5'-UUCUCCGAA CGUGUCACGUTT -3', antisense strand: 5'-ACGUGACAC GUUCGGAGAATT-3'), miR-590-3p mimic (miR-590-3p: 5'-TAATTTTATGTATAAGCTAGT-3') and the negative control (NC: 5'-UUCUCCGAACGUGUCACGUTT-3') mimic, miR-590-3p inhibitor (anti-miR-590-3p: 5'-ACTAGCTTATAC ATAAAATTA-3') and the NC inhibitor (anti-NC: 5'-CAG UACUUUUGUGUAGUACAA-3'), MALAT1 overexpression vector (MALAT1) and the empty pcDNA3.1 vector (Vector; Invitrogen; Thermo Fisher Scientific, Inc.) were purchased from Guangzhou RiboBio Co., Ltd. Cell transfection was performed using Lipofectamine® 2000 reagent (Invitrogen; Thermo Fisher Scientific, Inc.). When cell confluence reached ~90%, a mixture of 0.8 μg plasmid or 20 nM oligonucleotides and 2 μl Lipofectamine was added to each well of the 96-well plate and incubated in a CO_2 incubator at 37˚C, followed by incubation for 48 h. Meanwhile, untreated cells acted as the Control group.

RT-qPCR. Total RNA was extracted from tissues and cell lines (hFOB1.19, and OS cell lines HOS, U2OS, 143B and MG-63) using TRIzol® reagent (Invitrogen; Thermo Fisher Scientific, Inc.). RNA was reversely transcribed into cDNA using the High-Capacity cDNA Reverse Transcription Kit (Thermo Fisher Scientific, Inc.) or MicroRNA Reverse Transcription Kit (Thermo Fisher Scientific, Inc.), according to the manufacturer's protocols. The expression levels were detected using SYBR® Premix Ex Taq™ (Takara Biotechnology Co., Ltd.) and quantified using $2^{-\Delta\Delta Cq}$ method. GAPDH and U6 were used as internal references. Primer sequences were as follows: MALAT1-forward (F), 5'-AAAGCAAGGTCTCCCCAC AAG-3' and MALAT1-reverse (R), 5'-GGTCTGTGCTAG ATCAAAAGGCA-3'; miR-590-3p-F, 5'-GCGTAATTTTAT GTATAAGC-3' and miR-590-3p-R, 5'-GTATCCAGTGCG TGTCGTGGAGT-3'; GAPDH-F, 5'-GACTCCACTCACGGC AAATTCA-3' and GAPDH-R, 5'-TCGCTCCTGGAAGAT GGTGAT-3'); U6-F, 5'-CTCGCTTCGGCAGCACA-3' and U6-R, 5'-AACGCTTCACGAATTTGCGT-3'.

Cell Counting Kit-8 (CCK-8) assay. A total of $2x10^3$ 143B and MG-63 cells were seeded into 96-well plates (Corning, Inc.) after transfection. A final 10% concentration of the CCK-8 solution (Dojindo Laboratories, Inc.) was added to each well after incubation for 24, 48 and 72 h. After 2 h incubation at 37˚C, the absorbance was measured at 450 nm using a microplate reader (Bio-Rad Laboratories, Inc.).

Cell apoptotic assay. Briefly, 143B and MG-63 cells ($1x10^6$) were digested with trypsin and washed with PBS. After being resuspended with binding buffer, the cells were stained with an Annexin V-FITC/PI kit (BD Pharmingen; BD Biosciences) for 15 min at room temperature in the dark. Then, the apoptotic rate was determined by the FACScan flow cytometry (BD Biosciences) and analyzed using FlowJo v.10.1 (FlowJo, LLC).

Transwell assay. For cell migration assay, the transfected 143B and MG-63 cells ($5x10^4$ cell/well) were seeded in serum-free DMEM and plated into the upper chamber of a 24-well Transwell with 8-μm polycarbonate membrane filters (Corning, Inc.). DMEM containing 10% FBS was added to the lower chamber. Cells were incubated for 24 h in a humidified atmosphere of 5% CO_2 at 37˚C. The cells adhering to the lower surface were fixed using 4% paraformaldehyde at 37˚C for 20 min, stained with 1% crystal violet at 37˚C for 10 min and counted under a light microscope (200x magnification; Olympus Corporation) in three random fields. For the invasion assay, the upper layer of the polycarbonate membrane was coated with 100 μl of diluted (1:1) Matrigel (BD Biosciences) and incubated at 37˚C for 4 h to dry into a gel. The invasive cells were analyzed using the same methods as aforementioned.

Western blot assay. Total protein was extracted from 143B and MG-63 cells using RIPA buffer (Thermo Fisher Scientific, Inc.). Proteins were quantified using BCA Protein Assay Kit (Pierce; Thermo Fisher Scientific, Inc.). A total of 50 μg protein was separated by SDS-PAGE on 10% gels and transferred to PVDF membranes (MilliporeSigma). The membranes were blocked with 5% skim milk for 2 h at room temperature and then incubated overnight at 4˚C with primary

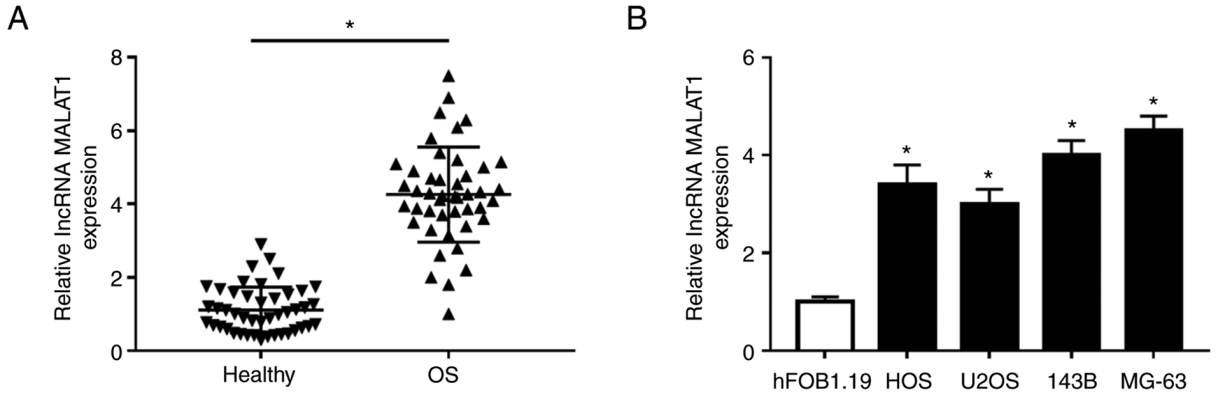

Figure 1. MALAT1 is upregulated in OS tissues and cells. (A) Reverse transcription-quantitative PCR assay was performed to measure the expression of MALAT1 in OS tissues and adjacent healthy tissues. (B) The level of MALAT1 was detected in OS cells (HOS, U2OS, 143B and MG-63) and human fetal osteoblastic cells (hFOB1.19). *P<0.05 as indicated or vs. hFOB1.19. OS, osteosarcoma; lncRNA, long non-coding RNA.

antibodies against E-cadherin (cat. no. ab40772), Vimentin (cat. no. ab92547), N-cadherin (cat. no. ab76011), Snail (cat. no. ab216347) and GAPDH (cat. no. ab9485) (all 1:2,000; all from Abcam). The membranes were washed twice in TBS-1% Tween 20 and incubated with horseradish peroxidase-conjugated goat-anti-rabbit secondary antibody (cat. no. ab97051; 1:100,000; Abcam) for 2 h at room temperature. Finally, the protein bands were detected using an ECL system (Pierce; Thermo Fisher Scientific, Inc.), and the intensity of the target protein was determined by ImageJ software v1.8.2 (National Institutes of Health). GAPDH was used as an internal reference.

Luciferase reporter assay. The binding sequences of MALAT1 and miR-590-3p were predicted using online software starBase v2.0 (https://starbase.sysu.edu.cn/). The sequences of wild-type (wt) MALAT1 (MALAT1-wt) and mutant (mut) MALAT1 (MALAT1-mut1 and MALAT1-mut2) containing miR-590-3p binding sites were cloned into pGL3 luciferase reporter vector (Promega Corporation). Then, pGL3 luciferase reporter vectors were co-transfected with miR-590-3p or NC into 143B and MG-63 cells using Lipofectamine 2000. Luciferase activity was examined using Dual-Luciferase Reporter Assay System (Promega Corporation) at 48 h after transfection according to the manufacturer's instructions. The activity of *Renilla* luciferase was used for normalization.

RNA immunoprecipitation (RIP) assay. RIP was performed with EZ-Magna RNA-Binding Protein Immunoprecipitation Kit (car. no. 17-701; MilliporeSigma) in accordance with the manufacturer's protocol. Briefly, 143B and MG-63 cells were transfected as aforementioned with miR-590-3p or NC, lysed at 4˚C using RIP lysis buffer for 5 min, and then incubated overnight at 4˚C with magnetic beads conjugated with argonaute 2 (AGO2; cat. no. ab186733; 1:50; Abcam) antibody. After purification from AGO2 immunoprecipitation complex, the relative MALAT1 expression was analyzed by RT-qPCR.

RNA pull-down assay. Biotin-labeled miR-590-3p probe (Bio-miR-590-3p) and the corresponding control probe (Bio-NC) were purchased from Guangzhou RiboBio Co., Ltd. In brief, the biotinylated probe at a final concentration of 100 nM was incubated with 100 μl M-280 Streptavidin Dynabeads (Invitrogen; Thermo Fisher Scientific, Inc.) at room temperature for 2 h to form probe-coated beads. Then, 143B and MG-63 cells were transfected with Bio-miR-590-3p or Bio-NC, according to the aforementioned protocol. Subsequently, the cells were lysed with Pierce IP lysis buffer (Thermo Fisher Scientific, Inc.) at 4˚C for 5 min and incubated with probe-coated beads at 4˚C for 3 h. After RNA isolation, the enrichment of MALAT1 was examined by RT-qPCR.

Statistical analysis. All data are presented as the mean ± standard deviation of three independent experiments. Pearson correlation analysis was used to analyze the association between the expression levels of MALAT1 and miR-590-3p in OS tissues. Statistical analysis was performed using unpaired or paired Student's t-test for two groups and one-way ANOVA followed by Turkey's post hoc test for multiple groups. Notably, the paired Student's t-test was used to compare tumor tissues and adjacent non-tumor tissues of the same patients. Statistical analysis was implemented using GraphPad Prism 7 software (GraphPad Software, Inc.). P<0.05 was considered to indicate a statistically significant difference.

Results

MALAT1 is upregulated in OS tissues and cells. To investigate the expression of MALAT1 in OS tissues and cells, RT-qPCR was performed in OS tissues and cell lines. The results demonstrated that MALAT1 was significantly increased in OS tissues compared with adjacent non-tumor tissues (Fig. 1A). Next, the expression of MALAT1 was significantly upregulated in OS cells (HOS, U2OS, 143B and MG-63) compared with human fetal osteoblastic cells (hFOB1.19) (Fig. 1B). These data suggested that dysregulation of MALAT1 may be associated with OS.

MALAT1 knockdown suppresses proliferation, migration, invasion and promotes apoptosis in OS cells. Loss-of-function experiments were performed to examine the function of MALAT1 in OS cell proliferation and apoptosis. Since the expression levels of MALAT1 were higher in the 143B and MG-63 cell lines than those in the other OS cell lines (HOS and U2OS), 143B and MG-63 cells were selected for

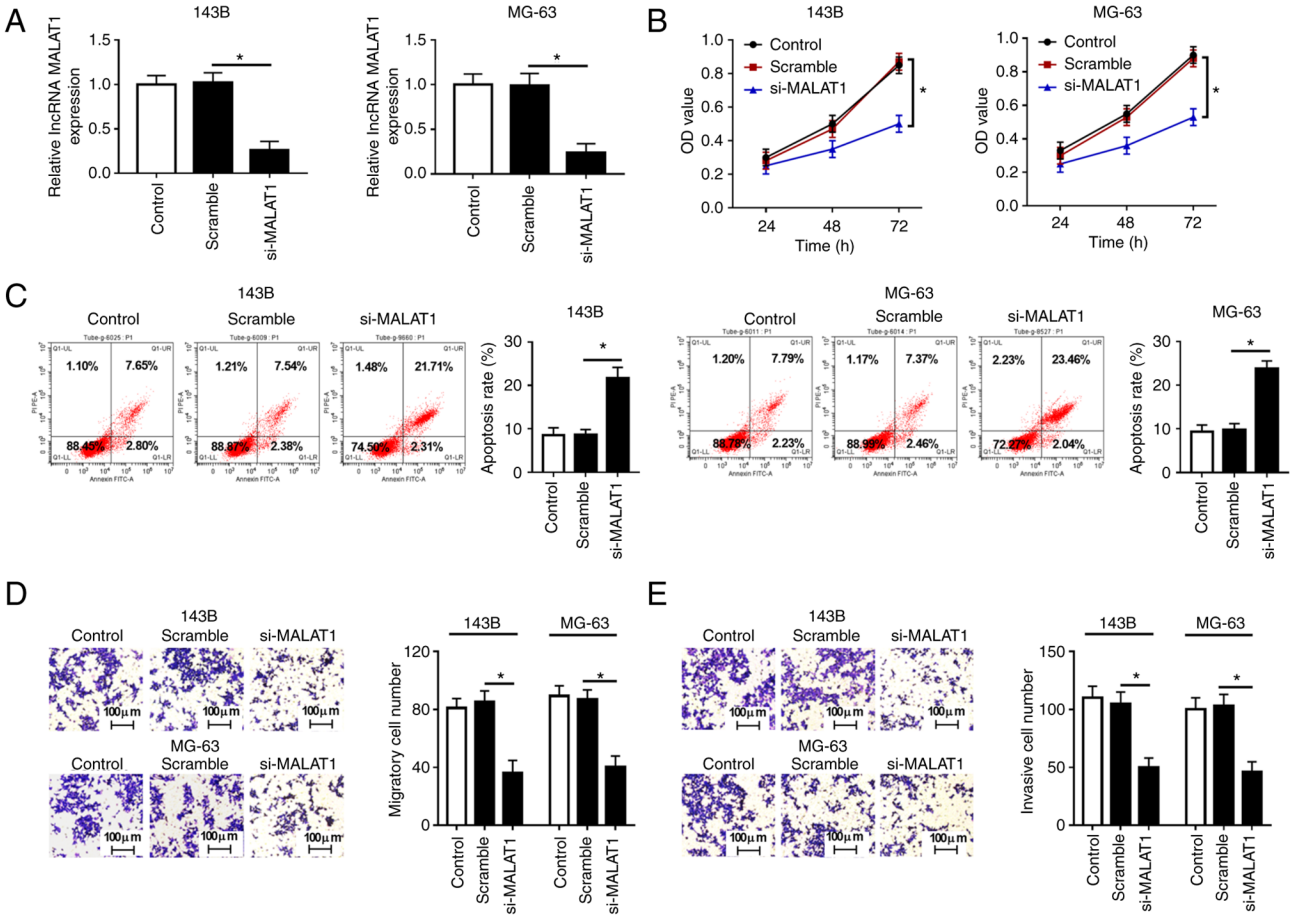

Figure 2. MALAT1 knockdown suppresses proliferation, migration, invasion and promotes apoptosis in osteosarcoma cells. 143B and MG-63 cells were transfected with Scramble or si-MALAT1. (A) MALAT1 expression was measured using reverse transcription-quantitative PCR in transfected cells. (B) Cell proliferative capacity was evaluated by Cell Counting Kit-8 assay at 24, 48 and 72 h after transfection. (C) Cell apoptotic rate was detected using flow cytometry at 48 h upon transfection. (D) Cell migration and (E) invasion were detected by Transwell assay. Scale bars, 100 μm. *P<0.05. si, small interfering; OD, optical density.

subsequent experiments. Firstly, the expression of MALAT1 was detected in 143B and MG-63 cells transfected with Scramble or si-MALAT1, and the results demonstrated that transfection with si-MALAT1 significantly decreased MALAT1 expression compared with Scramble (Fig. 2A). CCK-8 assay showed that MALAT1 knockdown significantly inhibited the proliferation of 143B and MG-63 cells (Fig. 2B). Flow cytometry assay revealed that the decrease of MALAT1 increased the apoptosis rate of 143B and MG-63 cells (Fig. 2C). Furthermore, Transwell assay demonstrated that MALAT1 knockdown markedly suppressed the migratory and invasive rate of 143B and MG-63 cells compared with cells transfected with Scramble (Fig. 2D and E). These results indicated that MALAT1 knockdown inhibited cell proliferation, migration and invasion, and induced apoptosis in OS cells.

MALAT1 knockdown inhibits EMT in OS cells. The effects of MALAT1 on EMT-related markers were determined using western blot assay. The results revealed that knockdown of MALAT1 increased the protein level of E-cadherin, and decreased the protein levels of N-cadherin, Vimentin and Snail in 143B and MG-63 cells transfected with si-MALAT1 compared with the Scramble group (Fig. 3A and B), which suggested that low levels of MALAT1 may inhibit EMT of OS cells.

Overexpression of miR-590-3p inhibits cell proliferation, migration, invasion and induces apoptosis in OS cells. Firstly, it was demonstrated that the expression of miR-590-3p was decreased in OS tissues compared with adjacent healthy tissues (Fig. 4A), and miR-590-3p was downregulated in HOS, U2OS, 143B and MG-63 cells compared with hFOB1.19 cells (Fig. 4B). After transfection of NC or miR-590-3p into 143B and MG-63 cells, the overexpression efficiency of miR-590-3p was determined by RT-qPCR (Fig. 4C). CCK-8 assay indicated that the proliferation of 143B and MG-63 cells was significantly inhibited in the miR-590-3p group compared with the NC group (Fig. 4D). Flow cytometry assay demonstrated that the apoptosis rate of both 143B and MG-63 cells transfected with miR-590-3p was increased (Fig. 4E and S1A). Transwell assay revealed that miR-590-3p overexpression markedly suppressed the migration and invasion of 143B and MG-63 cells (Fig. 4F and G; Fig. S1C and E). In addition, the protein level of E-cadherin was increased, and the protein levels of N-cadherin, Vimentin and Snail were decreased in 143B and MG-63 cells transfected with miR-590-3p compared with the NC group (Fig. 4H). These data suggested that miR-590-3p overexpression inhibited cell proliferation, migration, invasion and EMT, and induced apoptosis in OS cells.

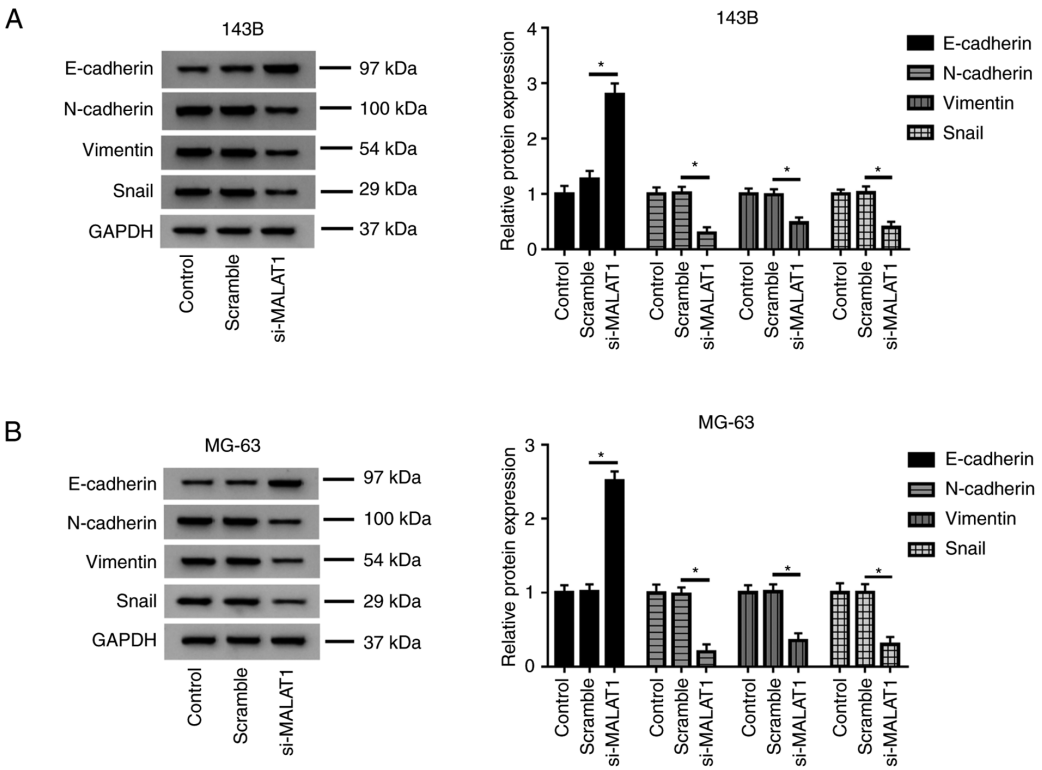

Figure 3. MALAT1 knockdown inhibits EMT in osteosarcoma cells. Levels of EMT-related proteins (E-cadherin, N-Cadherin, Vimentin and Snail) were examined by western blotting in (A) 143B and (B) MG-63 cells transfected with Scramble or si-MALAT1. *P<0.05. si, small interfering; EMT, epithelial-mesenchymal transition.

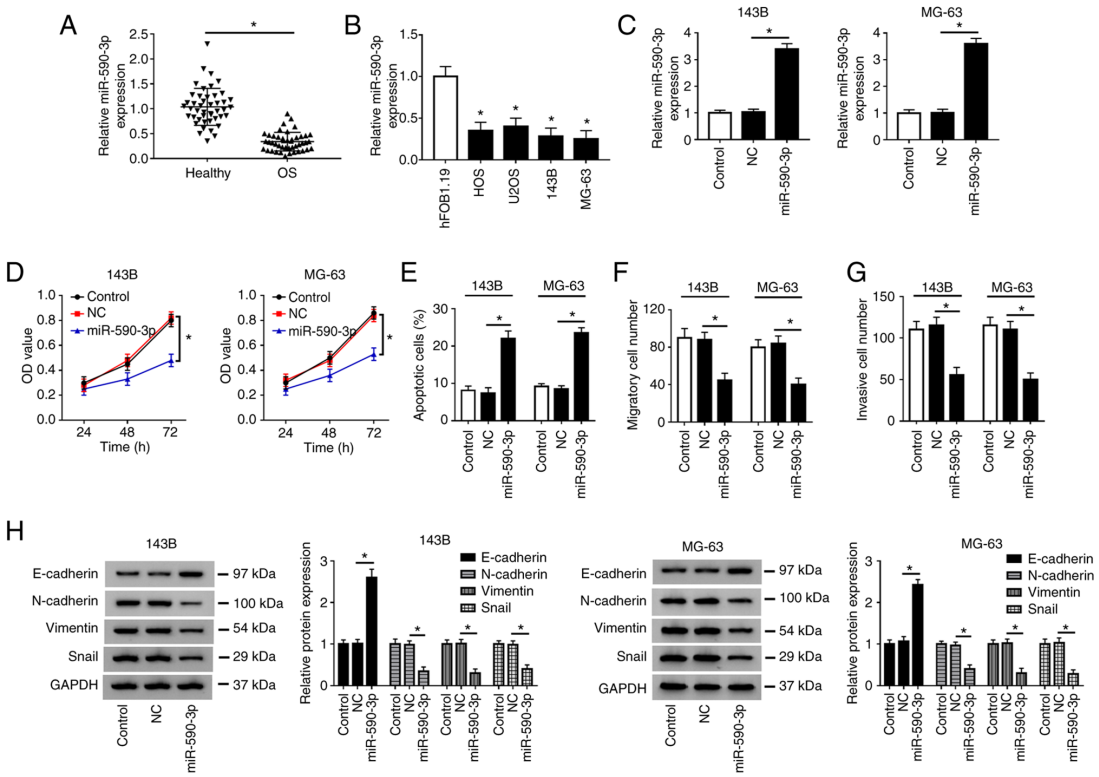

Figure 4. Overexpression of miR-590-3p inhibits cell proliferation, migration, invasion and induces apoptosis in OS cells. (A) Expression of miR-590-3p in OS tissues and adjacent healthy tissues was measured by RT-qPCR. (B) miR-590-3p expression was detected in OS cells (HOS, U2OS, 143B and MG-63) and human fetal osteoblastic cells (hFOB1.19). (C) miR-590-3p level was measured by RT-qPCR in 143B and MG-63 cells transfected with NC or miR-590-3p. (D) Cell proliferation was evaluated by Cell Counting Kit-8 assay at 24, 48 and 72 h after transfection. (E) Cell apoptotic rate was detected by flow cytometry. (F) Cell migration and (G) invasion were evaluated by Transwell assay. (H) Expression of epithelial-mesenchymal transition-related proteins (E-cadherin, N-Cadherin, Vimentin and Snail) was detected by western blotting. *P<0.05 as indicated or vs. hFOB1.19. RT-qPCR, reverse transcription-quantitative PCR; OD, optical density; miR, microRNA; NC, negative control; OS, osteosarcoma.

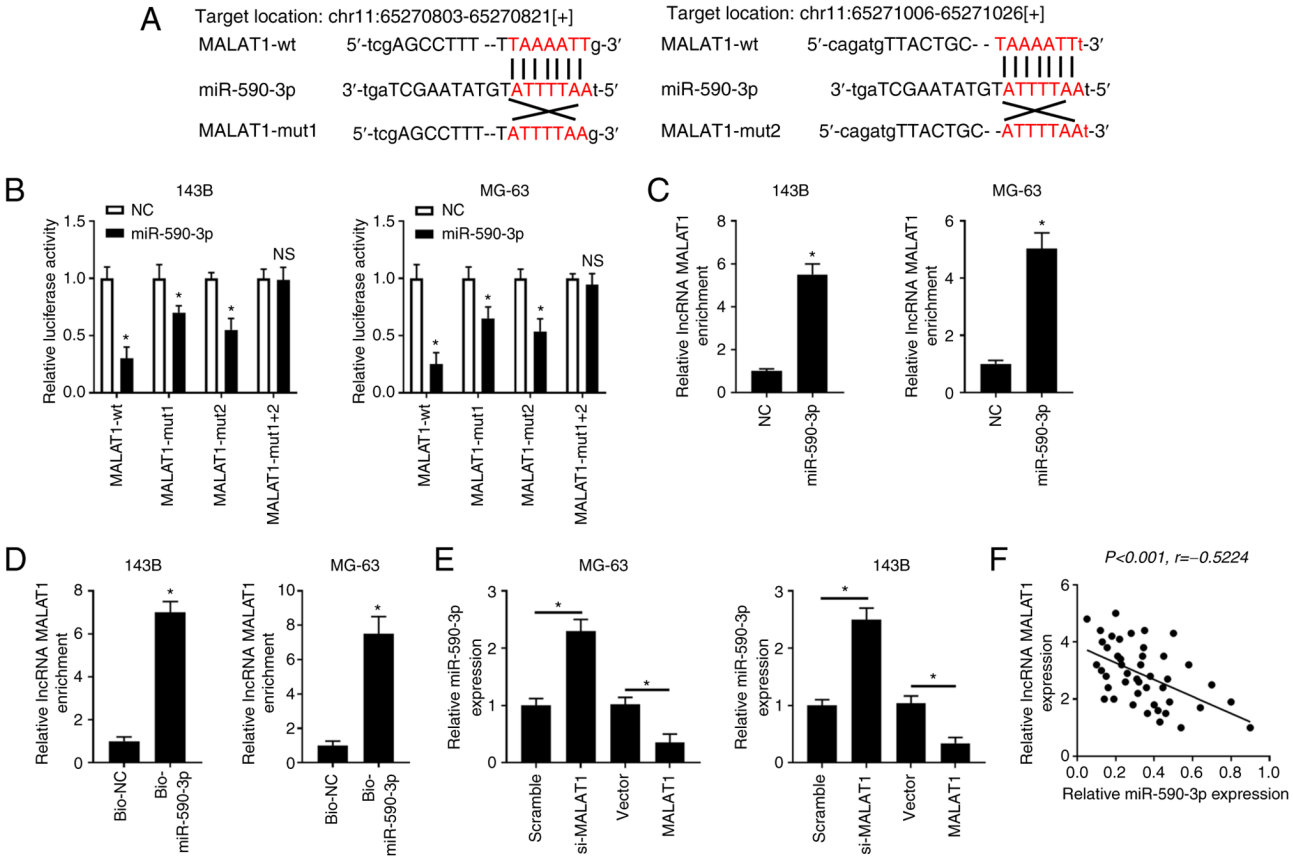

Figure 5. MALAT1 directly interacts with miR-590-3p. (A) Bioinformatics software predicted the putative binding sites between MALAT1 and miR-590-3p. (B) 143B and MG-63 cells were co-transfected with MALAT1-wt, MALAT1-mut1, MALAT1-mut2 or MALAT1-mut1+2 and miR-590-3p or NC, and the luciferase activity was examined at 48 h after transfection. (C) 143B and MG-63 cells were transfected with miR-590-3p or NC. RNA immunoprecipitation and RT-qPCR assays were performed to determine MALAT1 enrichment in AGO2 immunoprecipitation complex. (D) 143B and MG-63 cells were transfected with Bio-miR-590-3p or Bio-NC. RNA pull-down assay was carried out to detect MALAT1 enrichment. (E) 143B and MG-63 cells were transfected with Scramble, si-MALAT1, Vector or MALAT1. The levels of miR-590-3p were detected by RT-qPCR. (F) The correlation between MALAT1 and miR-590-3p in OS tissues was examined. *P<0.05. RT-qPCR, reverse transcription-quantitative PCR; miR, microRNA; NC, negative control; wt, wild-type; mut, mutant; si, small interfering; Bio, biotinylated; lncRNA, long non-coding RNA.

MALAT1 directly interacts with miR-590-3p. Bioinformatics software starBase v2.0 predicted the binding sites between MALAT1 and miR-590-3p (Fig. 5A). Luciferase reporter assay showed that miR-590-3p overexpression decreased the luciferase activity of MALAT1-wt in 143B and MG-63 cells, but failed to inhibit the luciferase activity of MALAT1-mut1+2 (Fig. 5B). Luciferase activity was also reduced in the MALAT1-mut1 and MALAT1-mut 2 groups, because both binding sites are active. Therefore, a single mutation in one of the binding sites allows miRNAs to bind to the unmutated site. Then, the specific binding between MALAT1 and miR-590-3p was validated using RIP and pull-down assays. RIP analysis showed that MALAT1 was notably enriched in the miR-590-3p group after precipitation with AGO2 antibody compared with the NC group (Fig. 5C). In addition, pull-down analysis revealed that MALAT1 was significantly enriched by binding to Bio-miR-590-3p, but not Bio-NC (Fig. 5D). Taken together, these results demonstrated that MALAT1 directly bound to miR-590-3p.

Next, the overexpression efficiency of MALAT1 was determined in 143B and MG-63 cells transfected with Vector or MALAT1 (Fig. S2A). The results showed that knockdown of MALAT1 markedly increased the expression of miR-590-3p in 143B and MG-63 cells compared with those in the Scramble group, whereas overexpression of MALAT1 notably reduced the expression of miR-590-3p in OS cells compared with in the control group (Vector) (Fig. 5E). Furthermore, the expression levels of MALAT1 and miR-590-3p were negatively correlated in OS tissues (Fig. 5F). These results indicated that MALAT1 negatively regulated miR-590-3p.

Knockdown of miR-590-3p reverses the effects of MALAT1 knockdown on the proliferation, apoptosis, migration, invasion and EMT of OS cells. To further explore the relationship between MALAT1 and miR-590-3p in OS, 143B and MG-63 cells were transfected with Scramble, si-MALAT1, si-MALAT1 + anti-NC and si-MALAT1 + anti-miR-590-3p, respectively. Firstly, the knockdown efficiency of anti-miR-590-3p was detected by RT-qPCR in 143B and MG-63 cells transfected with anti-NC or anti-miR-590-3p (Fig. S2B). Then, the results indicated that miR-590-3p was upregulated after knockdown of MALAT1, whereas miR-590-3p was markedly reduced after transfection with si-MALAT1 and anti-miR-590-3p (Fig. 6A). Knockdown of MALAT1 significantly suppressed cell proliferation (Fig. 6B), promoted apoptosis (Fig. 6C and S1B), and inhibited migration and invasion (Fig. 6D and E; Fig. S1D and F)

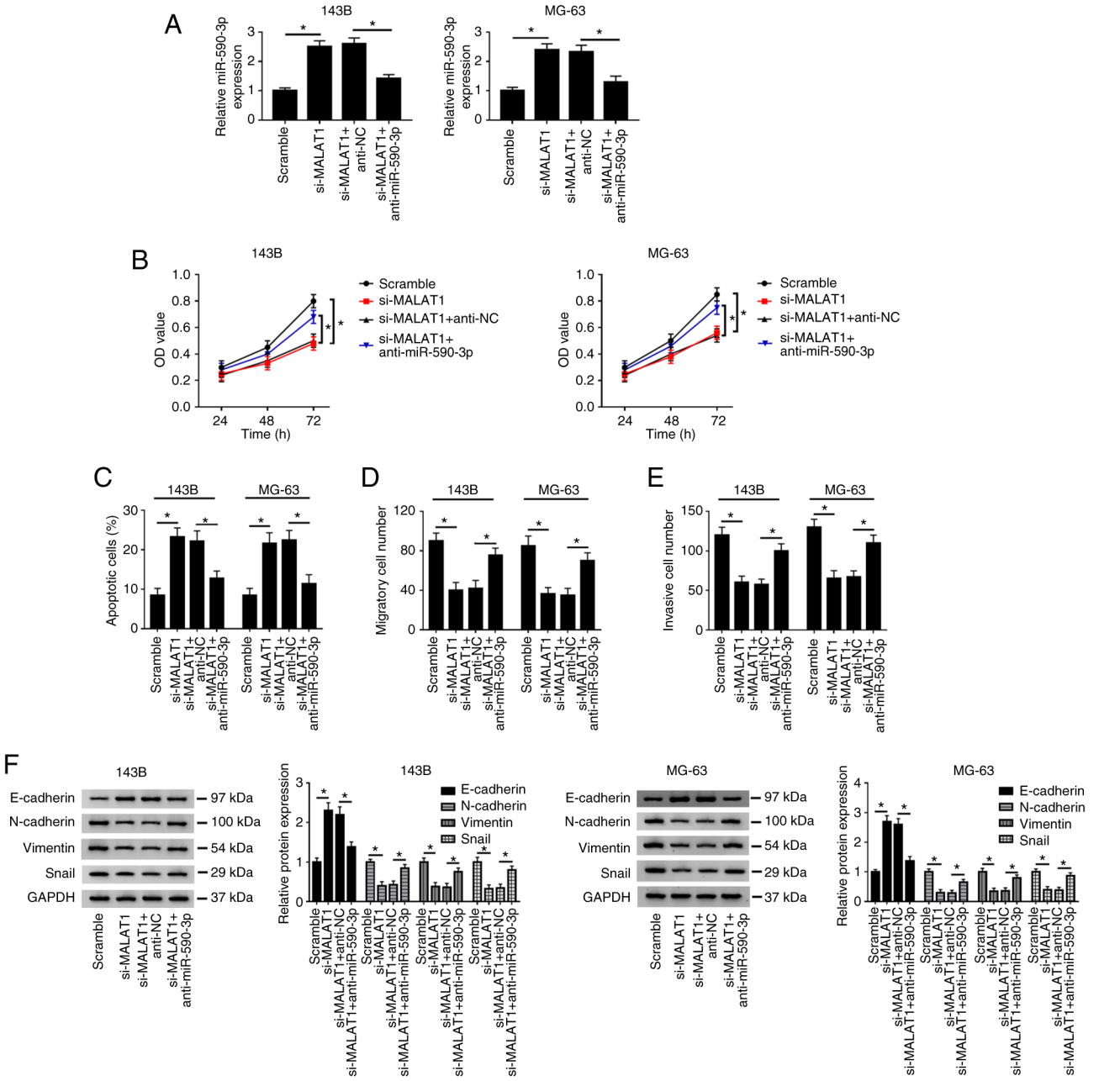

Figure 6. Inhibition of miR-590-3p reverses the effects of MALAT1 knockdown on the proliferation, apoptosis, migration, invasion and EMT of osteosarcoma cells. 143B and MG-63 cells were transfected with Scramble, si-MALAT1, si-MALAT1 + anti-NC and si-MALAT1 + anti-miR-590-3p. (A) miR-590-3p expression was measured by reverse transcription-quantitative PCR. (B) Cell proliferative capacity was evaluated by Cell Counting Kit-8 assay at 24, 48 and 72 h after transfection. (C) Cell apoptotic rate was detected by flow cytometry. (D) Cell migration and (E) invasion were evaluated by Transwell assay. (F) EMT-related protein (E-cadherin, N-Cadherin, Vimentin and Snail) expression was detected by western blotting. *P<0.05. EMT; epithelial-mesenchymal transition; miR, microRNA; NC, negative control; wt, wild-type; mut, mutant; si, small interfering; OD, optical density.

in 143B and MG-63 cells. In addition, 143B and MG-63 cells transfected with si-MALAT1 had higher E-cadherin protein level and lower N-cadherin, Vimentin and Snail protein levels compared with the Scramble group (Fig. 6F). However, these results caused by MALAT1 knockdown could be reversed by inhibiting miR-590-3p.

Discussion

It has been shown that numerous lncRNAs function as competitive endogenous RNAs (ceRNAs) in human tumors (23), including OS. For example, Wang *et al* confirmed that lncRNA HCG9 could contribute to OS growth through RAD51 by acting as a ceRNA of miR-34b-3p (8). In addition, Ding *et al* reported that lncRNA MELETF-AS1 may serve as a ceRNA of miR-485 to promote OS cell migration and invasion *in vitro* (10). Non-coding RNAs, including lncRNAs and miRNAs, could serve as potential tumor markers or therapeutic targets in OS (1). lncRNA MALAT1 has been reported to be an oncogenic factor in OS. For example, Ren *et al* (24) showed that MALAT1 knockdown suppressed cell proliferation by regulating CDK9 and competitively binding to miR-206 in OS. MALAT1 positively regulated cell proliferation, migration and invasion by sponging miR-34a/c-5p

and miR-449a/b in OS (25). Zhang *et al* (26) demonstrated that MALAT1 induced OS cell growth and metastasis, and inhibited cell apoptosis by modulating miR-509 to activate the Rac1/JNK pathway. Chen *et al* (27) found that MALAT1 increased stem cell-like properties and activated the PI3K/Akt signaling pathway by regulating Ret proto-oncogene and competitively binding to miR-129-5p. However, the molecular mechanisms of MALAT1 in OS cell proliferation, migration and invasion require further elucidation. Consistent with previous reports (24-27), in the present study MALAT1 was highly expressed in OS tissues and cell lines, and MALAT1 knockdown inhibited cell proliferation and triggered cell apoptosis in OS.

Accumulating evidence has demonstrated that ectopic expression of miRNAs plays an important role in metastasis, invasion and chemoresistance of human OS cells (28). miR-590-3p has been widely reported as a tumor suppressor in multiple malignant tumors, such as breast cancer (29), gastric cancer (30) and glioblastoma (31). However, miR-590-3p has been indicated to promote ovarian cancer cell proliferation, invasion and spheroid formation by targeting cyclin G2 and FOXO3 (32). In colon cancer cells, miR-590-3p positively regulated cell proliferation, spheroid formation and cell cycle by binding to Wnt inhibitory factor 1 and Dickkopf-related protein 1 (DKK1) (33). Wang *et al* (22) demonstrated that miR-590-3p may be a potential therapeutic target for OS by inhibiting SOX9 expression. Hu *et al* (34) found that RNA binding protein pumilio homolog 2 could inhibit OS cell progression by competitively binding to STARD13 with miR-590-3p and miR-9. The present study further demonstrated that miR-590-3p expression was significantly downregulated in OS tissues and cells compared with in adjacent healthy tissues and hFOB1.19 cells. Furthermore, it was demonstrated that MALAT1 negatively regulated miR-590-3p in OS tissues, and knockdown of miR-590-3p attenuated the inhibitory effect of MALAT1 on proliferation, migration and invasion and its promotive effect on apoptosis in OS cells. In addition, the current study revealed that MALAT1 directly bound to miR-590-3p. Bioinformatics analysis indicated that miR-590-3p and MALAT1 have two complementary sites. Moreover, the interaction between MALAT1 and miR-590-3p was verified by luciferase reporter, RIP and RNA pull-down assays.

In conclusion, the results of the present study indicated that MALAT1 promoted cell proliferation, migration, invasion and EMT and inhibited cell apoptosis by suppressing miR-590-3p in OS, which provided a promising therapeutic target or diagnostic marker for OS therapy. Due to the lack of in-depth analysis on tissue samples, the present study has certain limitations. Therefore, the effects of MALAT1 and miR-590-3p on OS progression require further investigation.

Acknowledgements

Not applicable.

Funding

No funding was received.

Availability of data and materials

All data generated or analyzed during this study are included in this published article.

Authors' contributions

HZ conceived and designed the study, and wrote the first draft of the manuscript. HZ, YW, WH, XD and WW performed all of the experiments. YW, WH, XD and WW analyzed and collated the results. HZ and YW confirm the authenticity of all the raw data. All authors read and approved the final manuscript.

Ethics approval and consent to participate

Written informed consent was obtained from all patients, and the research method was approved by the Ethics Committee of the First Hospital of Lanzhou University (Lanzhou, China).

Patient consent for publication

Not applicable.

Competing interests

The authors declare that they have no competing interests.

References

1. Luo Z, Xiao L, Li J, Dong B and Wang C: Integrative analysis reveals driver long non-coding RNAs in osteosarcoma. Medicine (Baltimore) 98: e14302, 2019.
2. Mirabello L, Troisi RJ and Savage SA: International osteosarcoma incidence patterns in children and adolescents, middle ages and elderly persons. Int J Cancer 125: 229-234, 2009.
3. Nie Z and Peng H: Osteosarcoma in patients below 25 years of age: An observational study of incidence, metastasis, treatment and outcomes. Oncol Lett 16: 6502-6514, 2018.
4. Luetke A, Meyers PA, Lewis I and Juergens H: Osteosarcoma treatment-where do we stand? A state of the art review. Cancer Treat Rev 40: 523-532, 2014.
5. Mercer TR, Dinger ME and Mattick JS: Long non-coding RNAs: Insights into functions. Nat Rev Genet 10: 155-159, 2009.
6. Zhang J, Hao X, Yin M, Xu T and Guo F: Long non-coding RNA in osteogenesis: A new world to be explored. Bone Joint Res 8: 73-80, 2019.
7. Li JP, Liu LH, Li J, Chen Y, Jiang XW, Ouyang YR, Liu YQ, Zhong H, Li H and Xiao T: Microarray expression profile of long noncoding RNAs in human osteosarcoma. Biochem Biophys Res Commun 433: 200-206, 2013.
8. Wang L, Li S, Qi L and Ling L: Long noncoding RNA HCG9 promotes osteosarcoma progression through RAD51 by acting as a ceRNA of miR-34b-3p. Mediators Inflamm: Aug 18, 2021 (Epub ahead of print).
9. Zhon Y, Feng D, Gu X, Gao A and Liu Y: The role and clinical significance of long noncoding RNA zinc finger E-box-binding homeobox two antisense RNA 1 in promoting osteosarcoma cancer cell proliferation, inhibiting apoptosis and increasing migration by regulating miR-145. Anticancer Drugs 32: 168-177, 2021.
10. Ding L, Liu T, Qu Y, Kang Z, Guo L, Zhang H, Jiang J, Qu F, Ge W and Zhang S: lncRNA MELTF-AS1 facilitates osteosarcoma metastasis by modulating MMP14 expression. Mol Ther Nucleic Acids 26: 787-797, 2021.
11. Chen R, Wang G, Zheng Y, Hua Y and Cai Z: Long non-coding RNAs in osteosarcoma. Oncotarget 8: 20462-20475, 2017.
12. Li ZX, Zhu QN, Zhang HB, Hu Y, Wang G and Zhu YS: MALAT1: A potential biomarker in cancer. Cancer Manag Res 10: 6757-6768, 2018.

13. Li Z, Yu X and Shen J: Long non-coding RNAs: Emerging players in osteosarcoma. Tumour Biol 37: 2811-2816, 2016.
14. Sun Y and Qin B: Long noncoding RNA MALAT1 regulates HDAC4-mediated proliferation and apoptosis via decoying of miR-140-5p in osteosarcoma cells. Cancer Med 7: 4584-4597, 2018.
15. Duan G, Zhang C, Xu C, Xu C, Zhang L and Zhang Y: Knockdown of MALAT1 inhibits osteosarcoma progression via regulating the miR34a/cyclin D1 axis. Int J Oncol 54: 17-28, 2019.
16. Lynam-Lennon N, Maher SG and Reynolds JV: The roles of microRNA in cancer and apoptosis. Biol Rev Camb Philos Soc 84: 55-71, 2009.
17. Di Leva G, Garofalo M and Croce CM: MicroRNAs in cancer. Annu Rev Pathol 9: 287-314, 2014.
18. Chen B, Xia Z, Deng YN, Yang Y, Zhang P, Zhu H, Xu N and Liang S: Emerging microRNA biomarkers for colorectal cancer diagnosis and prognosis. Open Biol 9: 180212, 2019.
19. Pang H, Zheng Y, Zhao Y, Xiu X and Wang J: miR-590-3p suppresses cancer cell migration, invasion and epithelial-mesenchymal transition in glioblastoma multiforme by targeting ZEB1 and ZEB2. Biochem Biophys Res Commun 468: 739-745, 2015.
20. Abdolvahabi Z, Nourbakhsh M, Hosseinkhani S, Hesari Z, Alipour M, Jafarzadeh M, Ghorbanhosseini SS, Seiri P, Yousefi Z, Yarahmadi S and Golpour P: MicroRNA-590-3P suppresses cell survival and triggers breast cancer cell apoptosis via targeting sirtuin-1 and deacetylation of p53. J Cell Biochem 120: 9356-9368, 2019.
21. Dou Y, Zhu K, Sun Z, Geng X and Fang Q: Screening of disorders associated with osteosarcoma by integrated network analysis. Biosci Rep: May 21, 2019 (Epub ahead of print).
22. Wang WT, Qi Q, Zhao P, Li CY, Yin XY and Yan RB: miR-590-3p is a novel microRNA which suppresses osteosarcoma progression by targeting SOX9. Biomed Pharmacother 107: 1763-1769, 2018.
23. Long J, Bai Y, Yang X, Lin J, Yang X, Wang D, He L, Zheng Y and Zhao H: Construction and comprehensive analysis of a ceRNA network to reveal potential prognostic biomarkers for hepatocellular carcinoma. Cancer Cell Int 19: 90, 2019.
24. Ren D, Zheng H, Fei S and Zhao JL: MALAT1 induces osteosarcoma progression by targeting miR-206/CDK9 axis. J Cell Physiol 234: 950-957, 2018.
25. Sun Z, Zhang T and Chen B: Long non-coding RNA metastasis-associated lung adenocarcinoma transcript 1 (MALAT1) promotes proliferation and metastasis of osteosarcoma cells by targeting c-Met and SOX4 via miR-34a/c-5p and miR-449a/b. Med Sci Monit 25: 1410-1422, 2019.
26. Zhang Y, Dai Q, Zeng F and Liu H: MALAT1 Promotes the proliferation and metastasis of osteosarcoma cells by activating the Rac1/JNK pathway via targeting MiR-509. Oncol Res: Apr 27, 2018 (Epub ahead of print).
27. Chen Y, Huang W, Sun W, Zheng B, Wang C, Luo Z, Wang J and Yan W: LncRNA MALAT1 promotes cancer metastasis in osteosarcoma via activation of the PI3K-Akt signaling pathway. Cell Physiol Biochem 51: 1313-1326, 2018.
28. Maximov VV, Akkawi R, Khawaled S, Salah Z, Jaber L, Barhoum A, Or O, Galasso M, Kurek KC, Yavin E and Aqeilan RI: MiR-16-1-3p and miR-16-2-3p possess strong tumor suppressive and antimetastatic properties in osteosarcoma. Int J Cancer 145: 3052-3063, 2019.
29. Rohini M, Gokulnath M, Miranda PJ and Selvamurugan N: miR-590-3p inhibits proliferation and promotes apoptosis by targeting activating transcription factor 3 in human breast cancer cells. Biochimie 154: 10-18, 2018.
30. Gu L, Lu LS, Zhou DL and Liu ZC: UCA1 promotes cell proliferation and invasion of gastric cancer by targeting CREB1 sponging to miR-590-3p. Cancer Med 7: 1253-1263, 2018.
31. Chen L, Wang W, Zhu S, Jin X, Wang J, Zhu J and Zhou Y: MicroRNA-590-3p enhances the radioresistance in glioblastoma cells by targeting LRIG1. Exp Ther Med 14: 1818-1824, 2017.
32. Salem M, Shan Y, Bernaudo S and Peng C: miR-590-3p targets cyclin G2 and FOXO3 to promote ovarian cancer cell proliferation, invasion, and spheroid formation. Int J Mol Sci 20: 1810, 2019.
33. Feng ZY, Xu XH, Cen DZ, Luo CY and Wu SB: miR-590-3p promotes colon cancer cell proliferation via Wnt/beta-catenin signaling pathway by inhibiting WIF1 and DKK1. Eur Rev Med Pharmacol Sci 21: 4844-4852, 2017.
34. Hu R, Zhu X, Chen C, Xu R, Li Y and Xu W: RNA-binding protein PUM2 suppresses osteosarcoma progression via partly and competitively binding to STARD13 3'UTR with miRNAs. Cell Prolif 51: e12508, 2018.